

RESEARCH

Open Access



The roles of a MiRNA and its targeted methyltransferase 3 in carotenoid accumulation in adductor muscles of QN orange scallops

Junlin Song¹, Xiao Sun¹ and Chunde Wang^{2,3*}

Abstract

Background QN Orange scallops are interspecific hybrids with orange adductor muscles that are rich in carotenoids. In this study, analysis of miRNA expression profiles was performed to explore possible regulatory patterns involved in carotenoid accumulation in adductor muscles of QN Orange scallops.

Results A total of 91 differentially expressed miRNA between the white and orange adductor muscles were identified. GO and KEGG analysis of target genes of differentially expressed miRNAs revealed enrichments in the transmembrane transporter activity-related pathways, kinase activity-related pathways, signal transduction-related pathways, ATP binding cassette transporters (ABC transporters), retinol metabolism, lipid-related metabolism, and calcium signaling pathway. In particular, miRNA Contig1462_36180, which was shown to negatively regulate the activity of methyltransferase 3 (METTL3) by dual-luciferase reporter assay, may play a pivotal role in the accumulation of carotenoids. Furthermore, METTL3 interference seemed to reduce the pectenoxanthin content and m6A level.

Conclusion It is thus speculated that Contig1462_36180 may regulate m6A methylation by regulating METTL3, which in turn affects pectenoxanthin accumulation in QN Orange scallops.

Keywords QN orange scallops, Carotenoid accumulation, MiRNA, Methyltransferase 3, N6-methyladenosine

Background

Color, as the primarily perceived organoleptic attribute, directly influences the selection of consumers [1]. Carotenoids are responsible for the yellow, orange, or red colors observed in marine organisms. In addition, carotenoids, as the source of provitamin A, benefit the health of marine organisms and humans [2]. Currently, carotenoid content has emerged as an important quality parameter and economic trait in seafood such as salmon [3].

Enormous efforts have been devoted to the exploration of the mechanism of carotenoid accumulation in marine organisms. In previous studies, genetic linkage

*Correspondence:

Chunde Wang
chundewang2007@163.com

¹Analysis and Testing Center, Qingdao Agricultural University, Qingdao 266109, China

²School of Marine Science and Engineering, Qingdao Agricultural University, Qingdao 266109, China

³Yantai Institute of Coastal Zone Research, Chinese Academy of Sciences, Yantai 264003, China



© The Author(s) 2025. **Open Access** This article is licensed under a Creative Commons Attribution-NonCommercial-NoDerivatives 4.0 International License, which permits any non-commercial use, sharing, distribution and reproduction in any medium or format, as long as you give appropriate credit to the original author(s) and the source, provide a link to the Creative Commons licence, and indicate if you modified the licensed material. You do not have permission under this licence to share adapted material derived from this article or parts of it. The images or other third party material in this article are included in the article's Creative Commons licence, unless indicated otherwise in a credit line to the material. If material is not included in the article's Creative Commons licence and your intended use is not permitted by statutory regulation or exceeds the permitted use, you will need to obtain permission directly from the copyright holder. To view a copy of this licence, visit <http://creativecommons.org/licenses/by-nc-nd/4.0/>.

map and quantitative trait loci mapping were extensively employed to investigate the mechanism of carotenoids accumulation in bivalve molluscs, such as the bay scallop (*Argopecten irradians*) [4], the Yesso scallop (*Patinopecten yessoensis*) [5] and the noble scallop (*Chlamys nobilis*) [6]. Genes associated with carotenoid accumulation, such as scavenger receptors, β -carotene15, 15'-monooxygenase and apolipoprotein (Apo), have been shown to play important roles in bivalve mollusks [7–9]. We also demonstrated that vacuolar protein sorting gene may play an important role in the accumulation of carotenoids in the QN Orange scallop [10].

Recent investigations have demonstrated that microRNAs (miRNAs) are also key regulatory factors in the mechanism of pigment accumulation in aquatic animals. For instance, miRNAs in leopard coral grouper (*Plectropomus leopardus*) [11], miR-138-5 and miR-722 in tilapia (*Oreochromis niloticus*) [12], and miR-137 in Manila clam (*Ruditapes philippinarum*) [13] have been found to be involved in body or shell color formation. Moreover, miRNA-430b has been shown to regulate *scarb1*, which is involved in carotenoid synthesis and coloration in Koi carp (*Cyprinus carpio* L.) [14]. Additionally, miR-15b was reported to target *hcApo*, which played essential roles in the carotenoid accumulation in *H. cumingii* [15]. However, whether miRNAs play roles in carotenoid accumulation in scallops remains unknown.

The predominant format of internal modification of mRNA is RNA methylation, which gives rise to N6-methyladenosine (m6A). m6A is a ubiquitous modification in mRNA and noncoding RNAs, affecting RNA splicing, translation, and stability, as well as the epigenetic effects of certain noncoding RNAs. It has emerged as a prevalent regulatory mechanism governing gene expression in various physiological processes [16]. Methyltransferase 3 (METTL3) is a major component of the m6A methyltransferase complex, which can catalyze the m6A modification of adenylate on mRNA [17]. Recent studies have shown that METTL3 can regulate biological processes through the regulation of m6A abundance in aquatic animals. In Zebrafish (*Danio rerio*), the absence of METTL3 resulted in failure in gamete maturation and compromised fertility, likely due to reduced m6A levels and disrupted expression of genes crucial for sex hormone synthesis and gonadotropin signaling [18]. In *Apostichopus japonicus*, METTL3 was found to modulate m6A signals and promote the translation of specific mRNA in response to the invasion of *Vibrio splendidus* [19]. It is known that m6A methylation in non-coding RNAs plays an important role in the coloration of plants [20–23]. In our previous RNA-seq libraries [24], many differentially expressed genes were enriched to pathways related to RNA methylation by GO analysis. However, whether METTL3 and m6A methylation are involved

in carotenoid accumulation in scallops has not been explored.

In our previous studies, we selected a new strain of scallop, namely QN Orange from the interspecific hybrids between the bay scallop (*Argopecten irradians irradians*) and the Peruvian scallop (*Argopecten purpuratus*) [25]. This new scallop strain is featured by its orange adductor muscles which is much appreciated by customers. Previous studies demonstrated the orange color in the adductor muscle of QN Orange scallops was due to the presence of pectenolone and pectenoxanthin [26]. In this study, we aimed to identify the potential miRNAs and their target genes that might contribute to QN Orange scallop adductor muscle coloration, based on miRNA analyses. Moreover, we sought to investigate the potential regulatory roles of m6A methylation in carotenoid accumulation. These findings may offer new insights into the regulatory mechanisms of carotenoid accumulation by miRNAs and m6A methylation of RNAs, thereby providing theoretical support for the breeding of new varieties with high content of carotenoids.

Methods

Animals

QN Orange scallops with orange adductor muscles (Group O) and Bohai Red scallops with white adductor muscles (Group W) were obtained from a scallop farm in Laizhou, Shandong Province, China. These scallops were subsequently transferred to the laboratory and adapted to laboratory conditions for at least 3 days before experiments. A total of nine adductor muscles from each strain were dissected and quickly frozen in liquid nitrogen for miRNA sequencing analysis. Adductor muscles from 3 animals were pooled together to form one sample for sequencing. In addition, 18 QN Orange scallops were randomly selected for the METTL3 inhibitor assay.

MiRNA library construction and sequencing

Total RNA from adductor muscle tissues was extracted using TRIzol reagent (Invitrogen, USA). Six small RNA libraries were constructed utilizing the Illumina TruSeq Small RNA kit (Illumina, USA). The small RNAs were ligated to 3' and 5' adapters, and reverse transcribed into cDNAs. Subsequently, PCR was employed for library enrichment. After library purification and cluster generation, sequencing was performed on Illumina Novaseq 6000 (Illumina, USA) to obtain raw data. High-quality clean reads (18 to 32nt) were then obtained by filtering out low-quality reads from the raw data and mapped to the *Argopecten irradians irradians* genome [27]. The mapped reads were aligned using the miRbase (<http://www.mirbase.org/>) and Rfam databases (<http://rfam.xfam.org/>) to identify the known miRNA and ncRNA, respectively. The miRDeep2 (<https://www.mdc-berlin.de/cont>

ent/mirdeep2-documentation) was employed to predict novel miRNA by exploring the secondary hairpin structure of the miRNA precursors.

The expression levels of miRNAs were calculated using Transcripts Per Million via a quantifier script in miRDeep2, and the differentially expressed miRNA was determined using the edgeR software with $|\log_2FC| \geq 1$ and $p\text{-value} < 0.05$.

Prediction of target mRNA for differentially expressed MiRNAs

The target mRNAs for differentially expressed miRNAs were predicted using miRanda (<http://www.miranda.org/>) and RNAhybrid (<http://bibiserv.techfak.uni-bielefeld.de/rnahybrid/>). To analyze the target mRNAs, Gene Ontology (GO) terms and Kyoto Encyclopedia of Genes and Genomes (KEGG) pathways were employed.

METTL3 inhibitor assay

STM2457 (Selleck, USA), a highly efficient and selective catalytic inhibitor on METTL3 [28], was diluted to 1 $\mu\text{g}/\mu\text{L}$ with PBS. A total of 18 QN Orange scallops were randomly divided into the experimental and vehicle groups. Each animal in the experimental group was injected with 150 μL STM2457 once each day for 3 consecutive days, while that in the vehicle group was injected with 150 μL of 1 \times PBS once each day for 3 consecutive days. The adductor muscles were then dissected and sampled for quantification of m6A methylation levels, measurement of carotenoid content, and real-time PCR, as detailed below.

Quantification of m6A RNA methylation

Total RNA was extracted from the adductor muscles with TRIzol Reagent (Invitrogen, CA, USA) and purified from total RNA using Oligo(dT) beads by MagicPure[®]mRNA Kit (EC511 TRAN, China). Then, 200ng purified mRNA was incubated with 2U nuclease P1 in 20 μL of a buffer containing 25mM NaCl and 1.5mM ZnCl_2 at 37 °C for 2 h. Subsequently, 3 μL of NH_4HCO_3 (1 M) and 1U alkaline phosphatase were added to the mixture, followed by a further incubation at 37 °C for 2 h. The resulted digestive product was diluted five-fold with deionized water and filtered through a 0.22 μm filter membrane.

N6 methyladenosine (>98%) and adenosine (>98%) were purchased from BeNa Culture Collection (Beijing, China). For calibration purposes, N6 methyladenosine

and adenosine were prepared at a concentration of 0.016 $\mu\text{g}/\text{L}$, 0.08 $\mu\text{g}/\text{L}$, 0.4 $\mu\text{g}/\text{L}$, 2 $\mu\text{g}/\text{L}$, 10 $\mu\text{g}/\text{L}$, 100 $\mu\text{g}/\text{L}$ and 1000 $\mu\text{g}/\text{L}$.

The m6A RNA methylation level was detected using an Ultra High Pressure Liquid Chromatography Tandem Mass Spectrometer (UHPLC-MS, 1290/6460 Agilent). The column used was the InfinityLab Poroshell 120 EC-C18 (50 \times 2.1 mm, 2.7 μm particle size, Agilent), with a column temperature of 30 °C. The LC gradient was generated using solvents A (methyl alcohol) and B (0.1% methanoic acid). The flow rate was 0.3 mL min^{-1} , and the injection volume was 2 μL . MS analysis was performed with Multiple Reaction Monitoring (MRM) of samples for sample detection in positive ion mode. Typical interface conditions were configured as follows: capillary voltage of 4 kV; source temperature at 350 °C; desolvation temperature set to 350 °C; desolvation gas flow rate of 12 L min^{-1} ; and sheath gas flow rate of 10 L min^{-1} . High purity nitrogen was utilized as the collision gas. The optimized mass parameters of N6 methyladenosine and adenosine were in Additional Table 1. The standard curve was constructed based on the concentration of the standard substance and the peak area, and the m6A/A ratio was calculated.

Measurement of carotenoids

Cold acetone (2.7 mL) was added to the freeze-dried adductor muscles (0.2 g) following ultrasonic treatment. The samples were then diluted with deionized water (0.2 mL), followed by freeze-drying for 12 h at -20 °C. After centrifugation and filtration, the contents of pectenolone and pectenoxanthin in the extracts were determined using an Ultra High Pressure Liquid Chromatography Tandem Mass Spectrometer (UHPLC-MS, 1290/6460 Agilent) with electrospray ionization (ESI) without standards. Chromatography was performed using an Infinity Lab Poroshell 120 EC-C18 column (i.d. 2.1 \times 50 mm, particle size 2.7 μm). The mobile phase consisted of acetonitrile (A) and 0.1% methanoic acid solution (B). The column temperature was set at 30 °C, and the flow rate was 0.3 mL min^{-1} . The injection volume was 2 μL . The HPLC-MS operated in the positive ionization mode with selected ion monitoring (SIM) relative quantification. The target quasi-molecular ions for pectenolone and pectenoxanthin were 581 and 565, respectively (Additional Fig. 1). The relative contents of pectenolone and pectenoxanthin were compared according to the peak area of SIM.

Quantitative real-time PCR assays

The expression levels of METTL3 mRNA were determined by quantitative real-time PCR (qRT-PCR). β -actin was used as an endogenous control. The primers for mRNA qRT-PCR are presented in Table 1. The

Table 1 Primer sequences used in RT-qPCR

Sample name	
METTL 3-F	CGACATGGAAACCTTCGTGC
METTL 3-R	TGGCTTGAGAGGGGAGACTT
β -actin-F	GCCGTGACTTGACCGATTACC
β -actin-R	CCTTGATGCCCTGACGATTTCTC

first-strand cDNA synthesis from RNA was conducted using TransScript® Uni All-in-One First-Strand cDNA Synthesis SuperMix for qPCR (AU341 TRAN China). Quantitative real time PCR reactions were performed utilizing PerfectStart® Green qPCR SuperMix (AQ601 TRAN China) on 450–725 nm CFX 96 Touch, according to the manufacturer’s instruction. The expression level of mRNA was calculated employing the 2^{^(-ΔΔCt)} method. Statistical significance was attributed to the expression level with a P value < 0.05.

Dual-luciferase reporter assay

The wild type and mutant sequences of METTL3 with XhoI and NotI restriction sites incorporated were synthesized. Subsequently, the synthetic sequence was cloned into the pmiR-RB-Report™ vector and amplified by PCR. The PCR purified products and vectors were double digested by XhoI and NotI, recovered and purified. After ligating the target fragments to the vectors, the transformation and colony PCR were performed. Finally, 48 h post-transfection of the plasmid into 293T cells, luciferase expression levels were assessed using the TransDetect® Double-Luciferase Reporter Assay Kit (FR201-01-V2 TRAN China).

Results

Expression of MiRNAs identified by deep sequencing

In total, 11,228,196 and 11,520,487 raw reads were generated from Group W (white adductor muscles) and Group O (orange adductor muscles), respectively (GEO accession number: GSE248569). After filtering, 10,948,600 (W) and 10,985,240 (O) clean reads remained. Among these reads, a total of 9,158,236 and 8,683,593 clean reads from the Group W and Group O samples were mapped to the bay scallop genome. Additionally, the Q20 values for clean reads were 98.69% (W) and 98.78% (O), while the Q30 values for clean reads were 96.12% (W) and 96.18% (O). Furthermore, the GC content was 43.6% in Group W and 45.68% in Group O (Table 2). There were 3289 miRNAs identified in both Group W and Group O, with 398 exclusively present in white adductor muscles, and 647 exclusively present only in orange adductor muscles (Fig. 1). In the Group W, a total of 3587 miRNAs were identified, including 3226 known miRNAs and 361 novel miRNAs. In the Group O, a total of 3936 miRNAs were identified, including 3606 known miRNAs and 331 novel miRNAs (Table 3).

Differentially expressed MiRNAs

A total of 91 differentially expressed miRNAs were identified between Group W and Group O, with 55 upregulated and 36 downregulated in orange adductor muscles (Padj ≤ 0.05, fold-change ≥ 2 or ≤ 0.5) (Fig. 2). Among these differentially expressed miRNAs, Contig220_8995 was

Table 2 Statistics of MiRNA sequences in white (W) and orange (O) adductor muscles

Sample	W	O
Raw reads	11,228,196.67	11,520,487
Raw bases	797,201,963.3	817,954,577
Clean reads	10,948,600.33	10,985,240.67
Q20(%)	98.69333333	98.78333333
Q30(%)	96.12666667	96.18333333
GC content(%)	43.59666667	45.68333333
Total reads	10,301,554.67	9,856,626
Total mapped	9158236.667	8683593.333

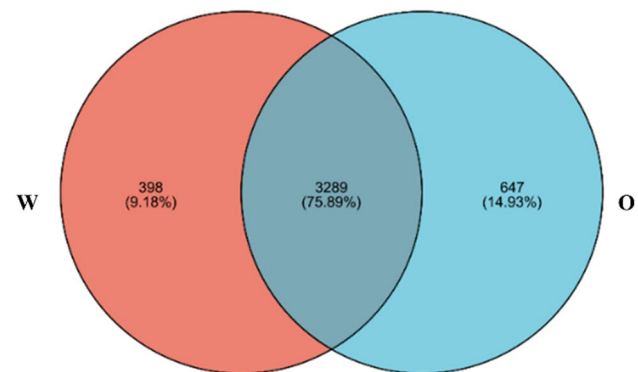


Fig. 1 The Venn analysis revealed the number of miRNAs in group W and group O and the overlapping relationship between miRNA genes in group W and group O. Orange-colored circles represent Group W, and the blue-colored circles represent Group O. The numerical values represent the number of common and unique miRNAs among white (W) and orange (O) adductor muscles

Table 3 Summary of MiRNA identification in white (W) and orange (O) adductor muscles

Sample groups	Known miRNA	Novel miRNA	Total miRNA
W	3226	361	3587
O	3606	331	3936

only one significantly down-regulated miRNA; while Contig2385_38971, Contig110_4495, and pma-miR-100b were significantly up-regulated miRNAs (Padj ≤ 0.01).

MiRNA target predictions and functional enrichment annotation

Among the 91 differentially expressed miRNAs, there were 3369 targets identified between Group W and Group O, while the four significant differentially expressed miRNAs, Contig220_8995, Contig2385_38971, Contig110_4495, and pma-miR-100b had 51 targets. In our previous RNA-seq libraries [24], we identified many differentially expressed genes between Group W and Group O related to RNA methylation, mRNA (guanine-N7-)-methyltransferase activity, and RNA methyltransferase activity (Additional Fig. 2). These results showed that RNA methylation may play a role in carotenoid accumulation. Notably, one target of Contig2385_38971

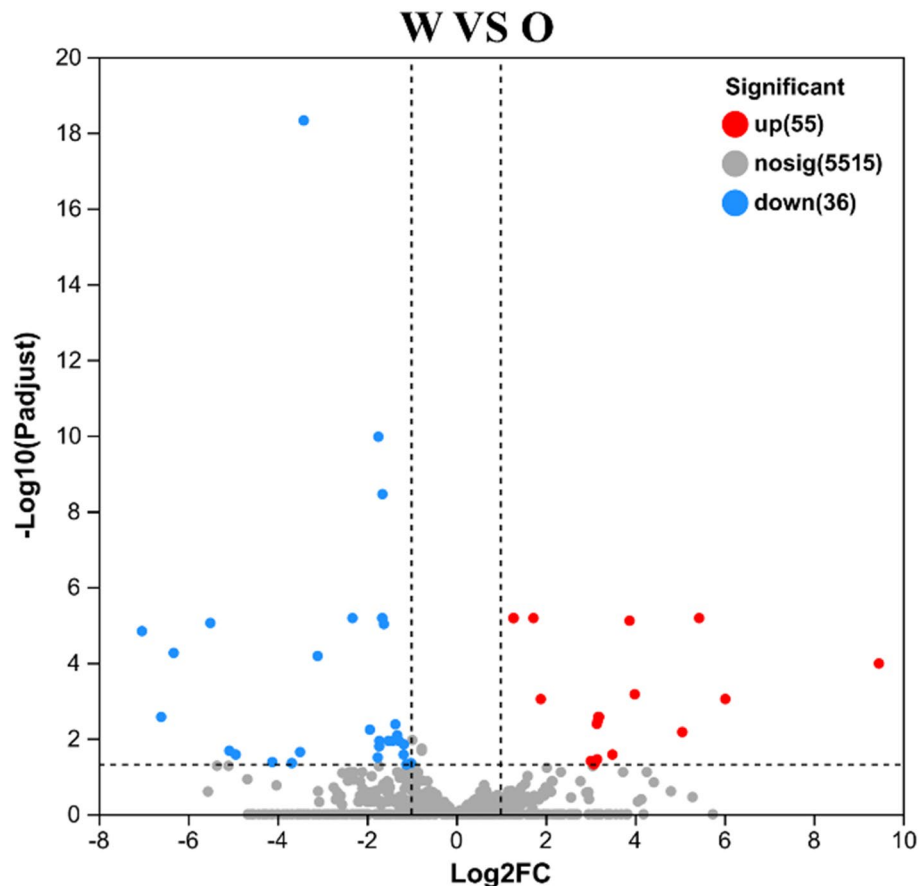


Fig. 2 Volcano plots for differentially expressed miRNAs between W vs. O. The red point represent up-regulated miRNAs, the blue points represent down-regulated miRNA, and the gray points represent no differential miRNAs

was methyltransferase domain. Additionally, Contig1462_36108 was only present in white samples, with one of its targets being methyltransferase 3 (METTL3).

GO enrichment analysis that these targets were significantly enriched in pathways related to transmembrane transporter activity, including purine-containing compound transmembrane transport, nucleotide transmembrane transport, plasma membrane protein complex, transmembrane receptor protein kinase activity, phosphate transmembrane transporter activity, transmembrane receptor protein tyrosine kinase activity, inorganic phosphate transmembrane transporter activity, and transmembrane receptor protein serine/threonine kinase activity. Additionally, kinase activity-related pathways were also enriched, such as MAP kinase kinase activity, receptor signaling protein serine/threonine kinase activity, protein tyrosine kinase activity, kinase activity, protein kinases activity and protein serine/threonine kinase activity. Furthermore, signal transduction-related pathways were identified, such as signal transduction and intracellular signal transduction (Fig. 3).

The KEGG enrichment analysis indicated that pathways related to carotenoid accumulation, such as ABC transporters, retinol metabolism, and lipid-related metabolism, were significantly enriched. Additionally, the calcium signaling pathway was also found to be enriched (Fig. 4).

The Inhibition of METTL3 decreased the carotenoid accumulation and mRNA m6A level in adductor muscles

STM2457 exhibits potent inhibition on the RNA methyltransferase METTL3 with high efficiency. The coloration of the adductor muscle in scallops treated with STM2457 and those treated with PBS was shown in Fig. 5. It can be seen that the adductor muscles of the QN Orange scallops treated with STM2457 were paler than those in the vehicle group. Meanwhile, as can be seen from Fig. 6a, the content of pectenoxanthin in adductor muscles from the vehicle group was higher than that in the STM2457-treated group ($P < 0.05$). However, no significant difference was observed in pectenolone content between the two groups ($P > 0.05$, Fig. 6b). As expected, mRNA levels of METTL3 were reduced in scallops treated with

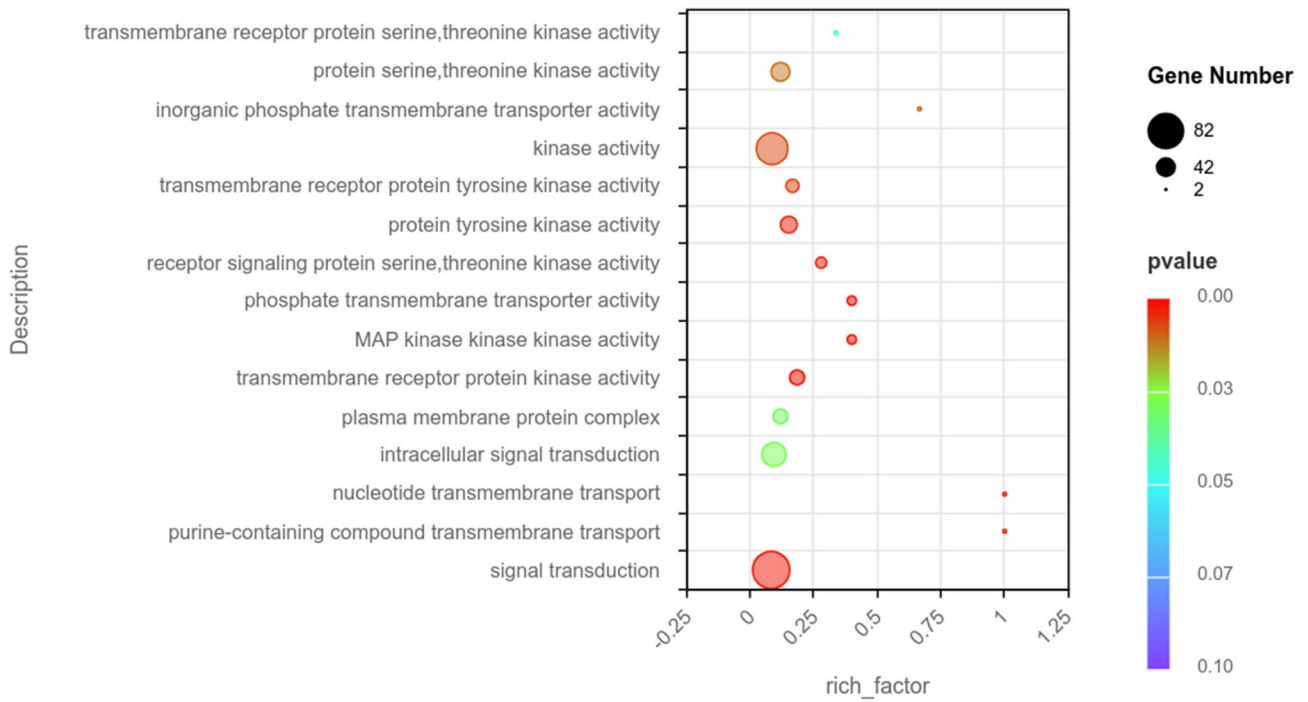


Fig. 3 Scatterplot of Go pathways related to stress response enriched the targets of differentially expressed miRNAs between the Group W and O

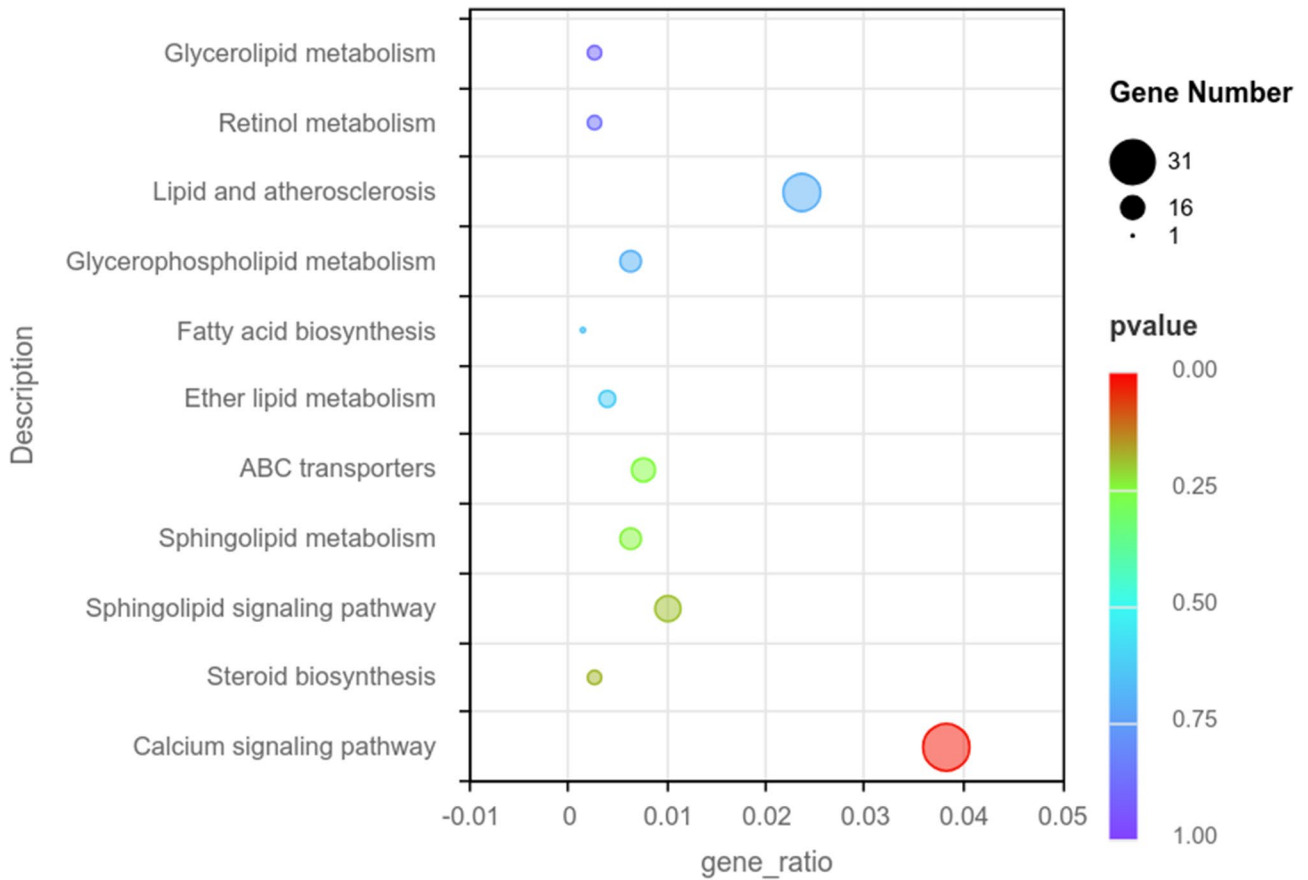


Fig. 4 Scatterplot of KEGG pathway related to carotenoid accumulation and the calcium signaling pathway enriched the targets of differentially expressed miRNAs between Group W and Group O

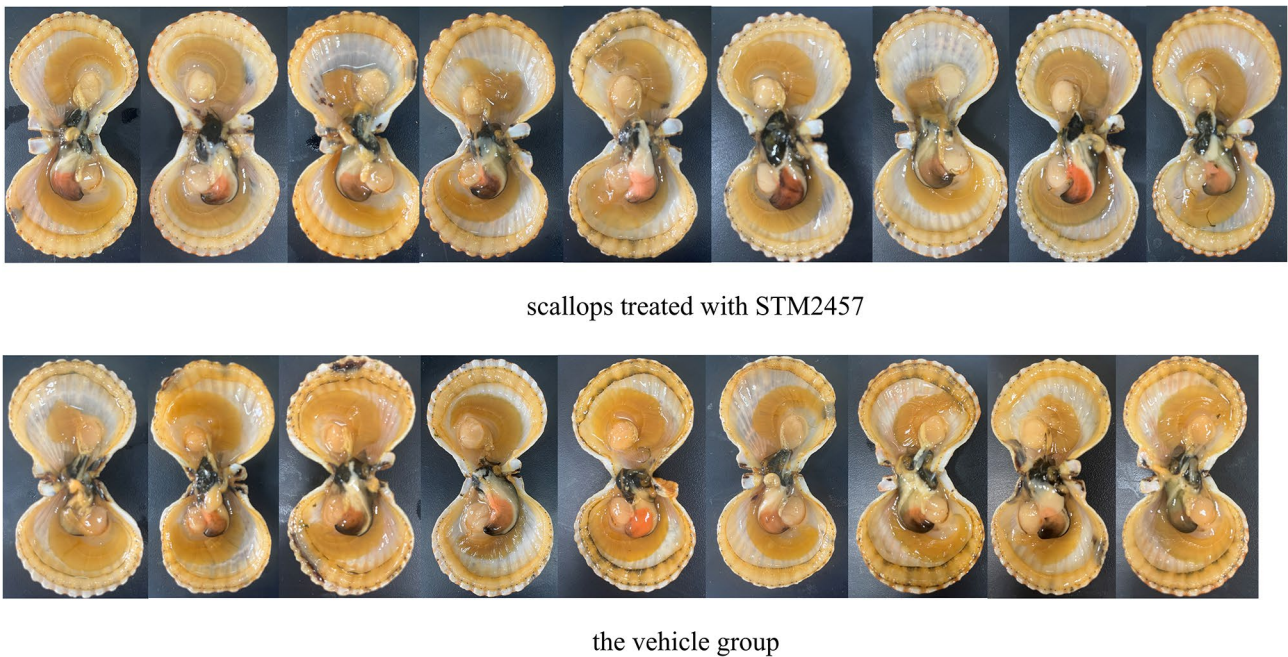


Fig. 5 The adductor muscles treated with STM2457 (upper panel) and the vehicle group treated with PBS (lower panel) in QN Orange scallops

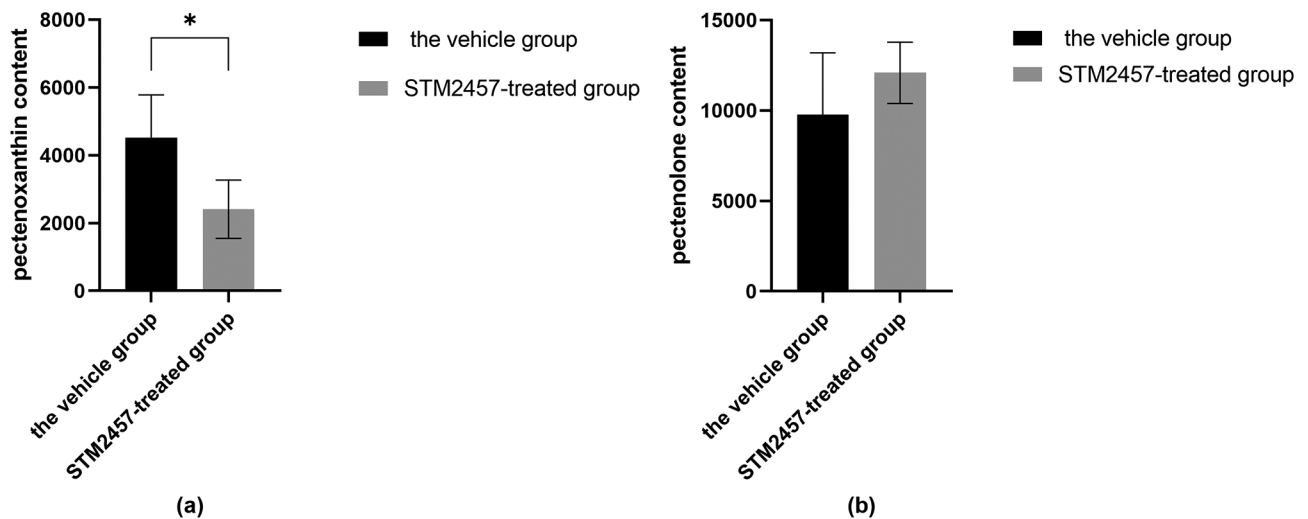


Fig. 6 The carotenoid content in QN Orange scallops with STM2457 and the vehicle group. The content of pectenoxanthin in adductor muscles from the STM2457-treated group and PBS-treated group (a) and the content of pectenolone in adductor muscles from the STM2457-treated group and PBS-treated group (b)

STM2457 along with a decrease in m6A levels (Figs. 7 and 8).

Dual-luciferase reporter assay

For METTL3 wild type (METTL3-WT) vector containing putative binding site of Contig1462_36180 was shown in Fig. 9a. And the mutations of METTL3 (METTL3-MUT) were shown in Fig. 9b. The luciferase activity of METTL3-WT was significantly reduced by Contig1462_36180 mimics, whereas no effect on the luciferase activity of METTL3-MUT was observed. This

provides evidence for the binding between METTL3 and Contig1462_36180 (Fig. 9c).

Discussion

miRNAs are short noncoding RNAs that regulate gene expression by binding to mRNAs of target genes [29]. It has been recognized that miRNAs target carotenoid transport and absorption genes. However, the mechanism of miRNAs coordinating carotenoid pigment has not been fully characterized. In this study, we sequenced all the miRNAs in the scallops with orange and white

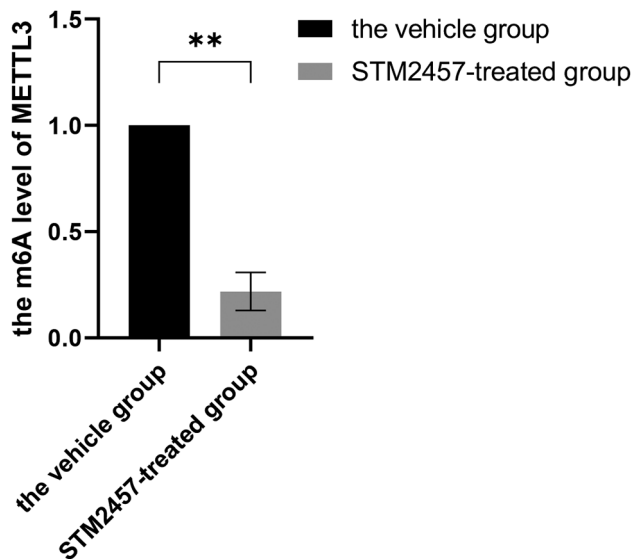


Fig. 7 mRNA levels of METTL3 in QN Orange scallops with STM2457 and the vehicle group

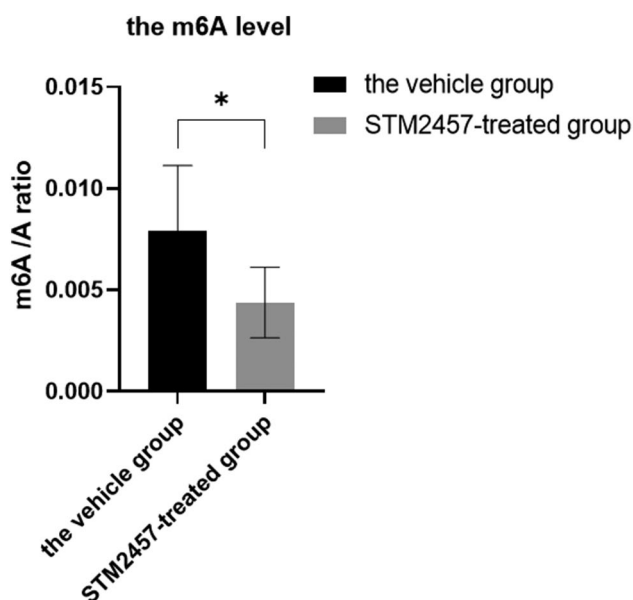


Fig. 8 m6A levels in QN Orange scallops with STM2457 and the vehicle group

adductor muscles and conducted enrichment pathways analysis of miRNAs target genes involved in carotenoid accumulation in orange adductor muscles. Interestingly, we discovered that Contig1462_36180 targets METTL3 in orange adductor muscles. Furthermore, we demonstrated that METTL3 regulates carotenoid accumulation through the modulation of m6A levels.

The KEGG enrichment analysis of the differentially expressed miRNA targets revealed significant involvement of ABC transporters, retinol metabolism, and lipid-related metabolism pathways. This observation can be

attributed to the accumulation of carotenoids in orange adductor muscles. In addition, GO and KEGG enrichment analysis revealed the involvement of certain targets in the calcium signaling pathway, pathways related to transmembrane transporter activity, kinase activity-related pathways, and signal transduction-related pathways. These pathways are integral components of the stress response mechanism, which can be attributed to the role of carotenoids in enhancing stress resistance. Essentially, stress triggers the activation of multiple signaling pathways through cell membrane receptors, subsequently leading to a cascade of stress responses. As natural antioxidants, carotenoids have been shown to improve physical condition and performance under various stressful conditions in marine animals. In the Caspian roach (*Rutilus caspicus*), dietary vitamin A has been found to enhance immune response [30]. High carotenoid content in Akoya pearl oysters (*Pinctada fucata*) has been demonstrated to increase resistance against high-temperature stress [31]. Carotenoids present in the gill tissue of Yesso scallops are believed to provide protection against oxidative stress [32]. Similarly, high levels of carotenoids have been shown to enhance immunity in noble scallops (*Chlamys nobilis*) [33]. Studies in crustaceans have indicated that supplementation with carotenoids improves various factors associated with stress tolerance [34].

The effects of m6A are determined by its readers, writers, and erasers. METTL3 is a crucial component of the m6A writer complex, which is indispensable for the formation of m6A [17]. METTL3 plays a pivotal role in regulating m6A methylation in a variety of biological processes. In *Saccharomyces cerevisiae*, deletion of the homologous gene to METTL3 resulted in reduced m6A methylation and developmental arrest specific to spores [35]. In *Arabidopsis thaliana*, the expression of the homologous gene to METTL3 was associated with m6A methylation and influenced growth and development traits [36]. METTL3 regulates the expression of m6A and downregulation of m6A methylation inhibits adipogenesis in porcine adipocytes [37]. Studies have shown that m6A methylation affects pigmentation in sheep skin [38]. This study demonstrates that STM2457 inhibits mRNA expression of METTL3, leading to decreased levels of carotenoid (pectenoxanthin) content and m6A modification. These results suggest that pectenoxanthin accumulation may be involved in the regulation of m6A methylation mediated by METTL3.

In our previous study, it was observed that the vacuolar protein sorting 29 gene (VPS29), a core component of the membrane transport complex Retromer, may lead to a reduction in pectenolone levels in orange adductor muscle with RNAi. However, VPS29 RNAi did not significantly affect the pectenoxanthin content [10]. In

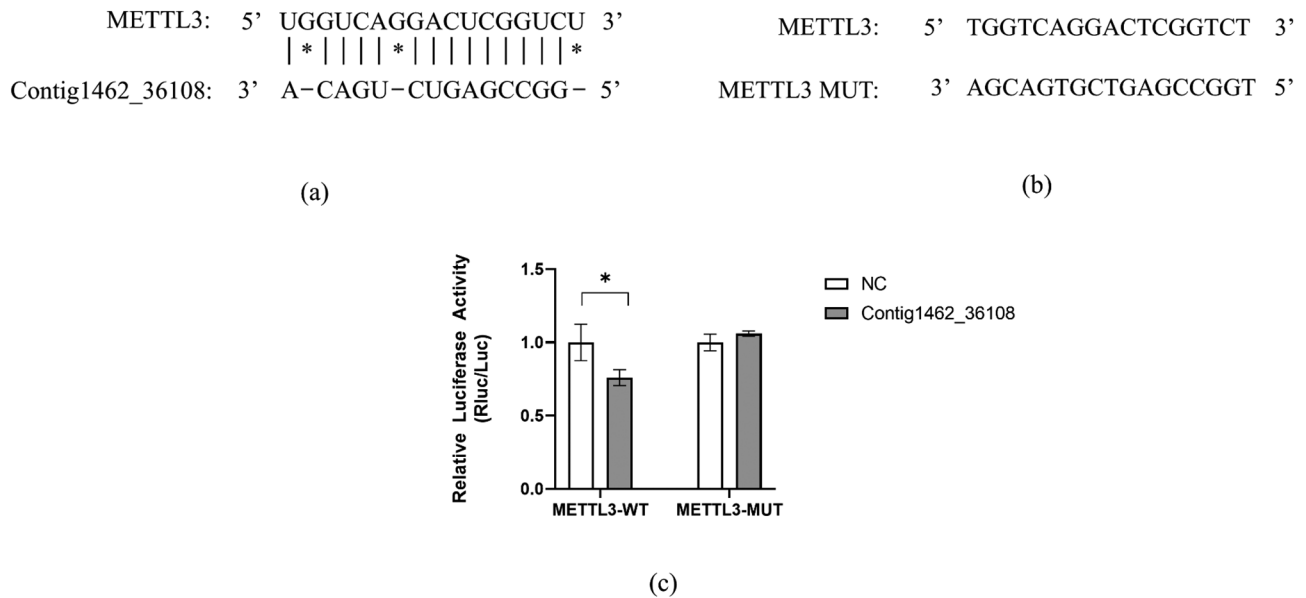


Fig. 9 Interaction between Contig1462_36180 and METTL3. The predicted binding sites of METTL3 and Contig1462_36180 (a), mutations (b) and the relative luminescence ratio by luciferase reporter assay (c)

this study, we found that blocking METTL3 resulted in a decrease in pectenoxanthin content, whereas no significant difference was observed in pectenolone content between the two groups. These findings suggest the accumulation of these two major carotenoids in orange muscle may be regulated by different pathways.

So far, a wide range of structurally diverse carotenoids have been discovered in marine animals. The distribution of these forms of carotenoids also varies among different species, life-history stages, developmental stages, and the organs or tissues of the animals. While common carotenoids such as β -carotene, astaxanthin, and lutein are widely present in many shellfish, pectenolone and pectenoxanthin are rare carotenoids that are exclusively found in scallops [26, 39]. For instance, abalones primarily accumulate zeaxanthin and β -carotene [40], while tridacnid clam (*Tridacna squamosal*) contains peridinin and pyrrhoxanthin [41]. Crustaceans and *Salmonidae* fishes predominantly amass astaxanthin [34], whereas tunaxanthin is widely distributed among *Perciformes* fishes [1]. In addition, carotenoid content varies among different tissues of the same species. For instance, in the red devil fish (*Cichlasoma citrinellum*), the astaxanthin content in the gonad is significantly higher compared to that in the skin and muscle [42]. The head and carapace of *P. stylifera* exhibit the highest total carotenoid contents, whereas *P. indicus* shows relatively lower levels of carotenoids in its body components [43]. Furthermore, there are significant differences in the percentage of carotenoids found in various tissues of pearl oyster [44]. On the other hand, different forms of carotenoids also show variations across tissues. In the previous study in

the 'QN Orange' scallops, α -carotene, β -carotene, and ζ -carotene were exclusively detected in gills and mantle, while canthaxanthin, pectenolone, pectenoxanthin, fucoxanthin, zeaxanthin, and lutein were present primarily within adductor muscles as well as gills and mantles [26].

The accumulation of specific carotenoids in various species or tissues implies that carotenoids can be targeted and transported to specific species or tissues. Research provided evidence that two strains of silkworm (*Bombyx mori*), SCR15 and Cameo2 were responsible for the transport of β -carotene and lutein to the two silk gland tissues, respectively [45]. These selective mechanisms and regulatory factors are worthy of further investigation.

Conclusion

In conclusion, we have identified differentially expressed miRNAs associated with carotenoid accumulation and further investigated the regulatory role of METTL3 in m6A modification during carotenoid metabolism. Our analysis of target genes based on small RNA sequencing data suggests that these differentially expressed miRNAs may play a role in regulating carotenoid accumulation and stress response. Notably, Contig1462_36108, was found to be negatively correlated with METTL3 expression. Furthermore, our findings indicate that METTL3 may reduce pectenoxanthin content in the adductor muscles of QN Orange scallops along with a decrease in m6A levels. These results provide additional evidence supporting the hypothesis that METTL3 is a crucial regulator involved in carotenoid-induced coloration in the adductor muscles of QN Orange scallops.

Abbreviations

ABC transporters	ATP binding cassette transporter
METTL3	Methyltransferase 3
Apo	Apolipoprotein
m6A	N6-methyladenosine
GO	Gene Ontology
KEGG	Kyoto Encyclopedia of Genes and Genomes
qRT-PCR	quantitative real-time
Group W	white adductor muscles
Group O	orange adductor muscles
VPS29	the Vacuolar Protein sorting 29 gene
METTL3-WT	METTL3 wild type
METTL3-MUT	The Mutations of METTL3

Supplementary Information

The online version contains supplementary material available at <https://doi.org/10.1186/s12864-025-11388-1>.

Supplementary Material 1

Supplementary Material 2

Supplementary Material 3

Acknowledgements

Not applicable.

Author contributions

JS designed the experiment, performed the analyses, and wrote the manuscript, XS participated in data processing, CW supervised the project and corrected the manuscript. All authors reviewed the manuscript.

Funding

This work was funded by the National Natural Science Foundation (Grant No. 32403000 and No. 31972791), the Shandong Province Natural Science Foundation (Grant No. ZR2024MC123), the Earmarked Fund for Agriculture Seed Improvement Project of Shandong Province (No. 2023LZGCQY006), and the Earmarked Fund for Shandong Modern Agro-Industry Technology Research System (No. SDAIT-14).

Data availability

Sequence data that support the findings of this study have been deposited in the GEO repository with the accession numbers GSE248569 and GSE122451.

Declarations**Ethics approval and consent to participate**

The scallops used in the current study were cultured by us, and we are allowed to use these materials for research. Since no endangered or protected species were involved in the experiments of this study, no specific permission was required for the animal material.

Consent for publication

Not applicable.

Competing interests

The authors declare no competing interests.

Received: 5 November 2024 / Accepted: 19 February 2025

Published online: 06 March 2025

References

- García-Chavarría M, Lara-Flores M. The use of carotenoid in aquaculture. *Res J Fish Hydrobiol.* 2013;8(2):38–49.
- Miyashita K, Hosokawa M. Health impact of marine carotenoids. *J Food Bioactives.* 2018;1:31–40.
- Sigurgisladdottir S, ØTorrissen O, Lie Ø, Thomassen M, Hafsteinsson H. Salmon quality: methods to determine the quality parameters. *Rev Fish Sci.* 1997;5(3):223–52.
- Du X, Song K, Wang J, Cong R, Li L, Zhang G. Draft genome and SNPs associated with carotenoid accumulation in adductor muscles of Bay scallop (*Argopecten irradians*). *J Genomics.* 2017;5:83–90.
- Wang S, Wang H, Zhao L, Zhang Y, Li T, Liu S et al. Identification of genes associated with carotenoids accumulation in scallop (*Patinopecten yessoensis*). *Aquaculture.* 2022;550:737850
- Ye T, Meng F, Tan K, Li L, Zhang G, Zheng H. Construction of genetic map and QTL analysis of carotenoid-related trait based on EST markers in noble scallop *Chlamys nobilis*. *Aquaculture.* 2021; 541:736775.
- Liu H, Zheng H, Zhang H, Deng L, Liu W, Wang S, et al. A de Novo transcriptome of the noble scallop, *Chlamys nobilis*, focusing on mining transcripts for carotenoid-based coloration. *BMC Genomics.* 2015;16(1):44–56.
- Huang Z, Guo X, Wang Q, Ma A, Zhao T, Qiao X, et al. Digital RNA-seq analysis of the cardiac transcriptome response to thermal stress in turbot *Scophthalmus maximus*. *J Therm Biol.* 2022;104:103141.
- Li X, Bai Z, Luo H, Liu Y, Wang G, Li J. Cloning, differential tissue expression of a novel HcApo gene, and its correlation with total carotenoid content in purple and white inner-shell color Pearl mussel *Hyriopsis cumingii*. *Gene.* 2014;538(2):258–65.
- Song J, Wang C. Transcriptomic and metabonomic analyses reveal roles of VPS 29 in carotenoid accumulation in adductor muscles of QN orange scallops. *Genomics.* 2021;113:2839–46.
- Hao R, Zhu X, Tian C, Jiang M, Huang Y, Zhu C. Integrated analysis of the role of miRNA-mRNA in determining different body colors of Leopard coral grouper (*Plectropomus leopardus*). *Aquaculture.* 2022;548:737575.
- Wang L, Zhu W, Dong Z, Song F, Dong J, Fu J. Comparative microRNA-seq analysis depicts candidate MiRNAs involved in skin color differentiation in red tilapia. *Int J Mol Sci.* 2018;19(4):1209–20.
- Ding J, Wen Q, Huo Z, Nie H, Qin Y, Yan X. Identification of shell-color-related MicroRNAs in the Manila clam *Ruditapes philippinarum* using high-throughput sequencing of small RNA transcriptomes. *Sci Rep.* 2021;11(1):1–8.
- Tian X, Peng N-n, Ma X, Wu L-m, Shi X, Liu H-f, et al. microRNA-430b targets scavenger receptor class B member 1 (scarb1) and inhibits coloration and carotenoid synthesis in Koi carp (*Cyprinus Carpio L*). *Aquaculture.* 2022;546:737334.
- Chen X, Bai Z, Li J. The mantle exosome and MicroRNAs of *Hyriopsis cumingii* involved in Nacre color formation. *Mar Biotechnol.* 2019;21(5):634–42.
- Zaccara S, Ries RJ, Jaffrey SR. Reading, writing and erasing mRNA methylation. *Nat Rev Mol Cell Biol.* 2019;20(10):608–24.
- Meyer KD, Jaffrey SR. Rethinking m(6A) readers, writers, and erasers. *Annu Rev Cell Dev Biol.* 2017;33:319–42.
- Xia H, Zhong C, Wu X, Chen J, Tao B, Xia X, et al. *Mettl3* mutation disrupts gamete maturation and reduces fertility in zebrafish. *Genetics.* 2018;208(2):729–43.
- Shao Y, Duan X, Zhao X, Lv Z, Li C. Global N(6)-methyladenosine methylation analysis reveals the positive correlation between m(6A) modification and mRNA abundance during *Apostichopus japonicus* disease development. *Dev Comp Immunol.* 2022;133:104434.
- Sheikh AH, Tabassum N, Rawat A, Almeida Trapp M, Nawaz K, Hirt H. m6A RNA methylation counteracts dark-induced leaf senescence in Arabidopsis. *Plant Physiol.* 2024;194(4):2663–78.
- Zhang Y, Wang J, Ma W, Lu N, Fu P, Yang Y, et al. Transcriptome-wide m6A methylation in natural yellow leaf of *Catalpa fargesii*. *Front Plant Sci.* 2023;14:1167789.
- Zhou L, Tian S, Qin G. RNA methylomes reveal the m(6A)-mediated regulation of DNA demethylase gene SIDML2 in tomato fruit ripening. *Genome Biol.* 2019;20(1):156.
- Guo S, Zheng Y, Meng D, Zhao X, Sang Z, Tan J, et al. DNA and coding/non-coding RNA methylation analysis provide insights into tomato fruit ripening. *Plant J.* 2022;112(2):399–413.
- Song J, Wang C. Transcriptomic and proteomic analyses of genetic factors influencing adductor muscle coloration in QN orange scallops. *BMC Genomics.* 2019;20(1):363.
- Wang C, Liu B, Liu X, Ma B, Zhao Y, Zhao X et al. Selection of a new scallop strain, the Bohai red, from the hybrid between the Bay scallop and the Peruvian scallop. *Aquaculture.* 2017;479:250–5.
- Zhao Q, Chen J, Zhu S, Liu X, Ma B, Wang C, et al. Pigment profiling of 'QN orange' scallop and 'Bohai red' scallop adductor muscles by liquid

- chromatography coupled with triple quadrupole mass spectrometry. *Aquacult Nutr.* 2019;508:178–85.
27. Liu X, Li C, Chen M, Liu B, Yan X, Ning J et al. Draft genomes of two Atlantic Bay scallop subspecies *Argopecten l. radians l. radians* and *A. l. concentricus*. *Sci Data.* 2020;7(1):99.
 28. Zhang X, Yin H, Zhang X, Jiang X, Liu Y, Zhang H, et al. N6-methyladenosine modification governs liver glycogenesis by stabilizing the glycogen synthase 2 mRNA. *Nat Commun.* 2022;13(1):7038.
 29. Cai Y, Yu X, Hu S, Yu J. A brief review on the mechanisms of MiRNA regulation. *Genom Proteom Bioinf.* 2009;7(4):147–54.
 30. Sharifan M, Hajimoradloo A, Ghorbani R, Hoseinifar SH. Effects of dietary retinol acetate on growth performance, skin mucus immune responses and haematological parameters of Caspian Roach (*Rutilus caspicus*). *Aquacult Nutr.* 2017;23(5):893–8.
 31. Meng Z, Zhang B, Liu B, Li H, Fan S, Yu D. High carotenoids content can enhance resistance of selected *Pinctada fucata* families to high temperature stress. *Fish Shellfish Immunol.* 2017;61:211–8.
 32. Li X, Li N, Zhao L, Shi J, Wang S, Ning X, et al. Tissue distribution and seasonal accumulation of carotenoids in yesso scallop (*Mizuhopecten yessoensis*) with orange adductor muscle. *Food Chem.* 2022;367:130701.
 33. Lu Y, Zhang H, Cheng D, Liu H, Li S, Ma H, et al. A multi-CRD C-type lectin gene Cnlec-1 enhance the immunity response in noble scallop *Chlamys nobilis* with higher carotenoids contents through up-regulating under different immunostimulants. *Fish Shellfish Immun.* 2018;83:37–44.
 34. Wade NM, Gabaudan J, Glencross BD. A review of carotenoid utilisation and function in crustacean aquaculture. *Rev Aquac.* 2017;9(2):141–56.
 35. Clancy M, Shambaugh M, Timpote C, Bokar J. Induction of sporulation in *Saccharomyces cerevisiae* leads to the formation of N⁶-methyladenosine in mRNA: a potential mechanism for the activity of the IME4 gene. *Nucleic Acids Res.* 2002;30(20):4509–18.
 36. Ruzicka K, Zhang M, Campilho A, Bodi Z, Kashif M, Saleh M, et al. Identification of factors required for m(6) A mRNA methylation in *Arabidopsis* reveals a role for the conserved E3 ubiquitin ligase HAKAI. *New Phytol.* 2017;215(1):157–72.
 37. Wang X, Zhu L, Chen J, Wang Y. mRNA m(6)A methylation downregulates adipogenesis in Porcine adipocytes. *Biochem Biophys Res Commun.* 2015;459(2):201–7.
 38. Zhao Y, Meng J, Song X, An Q. m6A mRNA methylation analysis provides novel insights into pigmentation in sheep skin. *Epigenetics.* 2023;18(1):2230662.
 39. Li N, Hu J, Wang S, Cheng J, Hu X, Lu Z, et al. Isolation and identification of the main carotenoid pigment from the rare orange muscle of the yesso scallop. *Food Chem.* 2010;118(3):616–9.
 40. Wei X, Yang B, Zeng W, Tang B, Huang M, Luo X et al. Carotenoid accumulation in common and orange-muscle mutant of Abalone, *Haliotis gigantea*, fed with different macroalgae. *Aquacult Nutr.* 2022; 2022:1–10.
 41. Maoka T, Akimoto N, Tsushima M, Komemushi S, Mezaki T, Iwase F. Carotenoids in marine invertebrates living along the Kuroshio current Coast. *Mar Drugs.* 2011;9:1419–27.
 42. Pan CH, Chien YH. Effects of dietary supplementation of Alga *Haematococcus pluvialis* (Flotow), synthetic Astaxanthin and β -carotene on survival, growth, and pigment distribution of red devil, *Cichlasoma citrinellum* (Günther). *Aquac Res.* 2009;40(8):871–9.
 43. Sachindra NM, Bhaskar N, Mahendrakar NS. Carotenoids in different body components of Indian shrimps. *J Sci Food Agr.* 2005;85(1):167–72.
 44. Zhang B, Zhu C, Meng Z, Liu B, Zhong L, Huang G et al. Carotenoids in Pearl oyster *Pinctada fucata*: the tissue distribution and correlation to color parameters. *Pak J Zoo.* 2019;51(5):1655–61.
 45. Takashi S, Seigo K, Tetsuya I, Junko N, Kimiko Y, Keiro U, et al. CD36 homolog divergence is responsible for the selectivity of carotenoid species migration to the silk gland of the silkworm *Bombyx mori*. *J Lipid Res.* 2013;4:482–95.

Publisher's note

Springer Nature remains neutral with regard to jurisdictional claims in published maps and institutional affiliations.